Associative plasticity of granule cell inputs to cerebellar Purkinje cells.

Rossella Conti and Céline Auger

SPPIN Saints-Pères Paris Institute for the Neurosciences, Université Paris Cité, CNRS,

F-75006 PARIS FRANCE

Abstract

Granule cells of the cerebellum make up to 175 000 excitatory synapses on a single Purkinje cell, encoding information from the mossy fibre inputs into the cerebellar cortex. The granule cell axon is made of an ascending portion and a long parallel fibre formed at right angle. There are controversial indications that ascending axon (AA) and parallel fibre (PF) synapse properties and modalities of plasticity are different. We tested the hypothesis that if AA and PF synapses are different, and encode different information, association of the inputs to Purkinje cells might be relevant to the circuit and might trigger plasticity, as does the coincident timing of parallel fibre and climbing fibre inputs. Here we describe a new form of associative plasticity between granule cell inputs. We show for the first time that AA and PF synchronous and repetitive train stimulation, with inhibition intact, triggers long term potentiation (LTP) at AA synapses and long term depression (LTD) at PF synapses. AA-LTP is associative and relies on the costimulation with PFs. AA-LTP is time dependent and the timing of presentation of the two inputs controls the outcome of plasticity. Finally, we show that both NMDAR and mGluR activation is required to induce AA-LTP. These observations reinforce the suggestion that AA and PF synapses are two synaptic populations with different coding capabilities and plasticity, governed by different modalities. Associative plasticity of AA and PF synapses enables effective association of different information, although both are transmitted via granule cells.

Introduction

The ability to discriminate self generated from external stimuli is essential to apprehend the world as movement itself activates sensory receptors. In fish, discrimination of self from external stimuli has been shown to rely on associating motor command and sensory feedback in cerebellar-like structures ((Montgomery & Bodznick, 1994); (Sawtell, 2017)). This is achieved by modifying the motor inputs to generate a negative image of the associated sensory inputs, effectively subtracting the predictable motor-associated sensory inputs so that only the unpredicted sensory inputs are output by the principal cells. While in most cases the role of the cerebellum in sensory information processing is still unclear, theoretical models and work on plasticity suggest that it might similarly be involved in cancellation of predictable sensory inputs, but distinct sensory and motor synapses have not yet been identified in the cerebellum. An intriguing possibility is that sensory and motor information inputs into the cerebellar cortex are morphologically separated from each other via the ascending axon and parallel fibers. If AA synapses relay motor information and play the role of local event detectors, as suggested by the work of Sims and Hartell (2005; 2006), functional association of AA and PF inputs, as observed in cerebellar-like structures, might produce different plasticity between the synapses depending on the relative timing of the two inputs.

Sensorimotor information is delivered to the cerebellar cortex by mossy fibres and relayed by granule cells to the Purkinje cells (PCs) and inhibitory network for integration. Anatomically, the axon of a granule cell first extends through the PC layer and into the molecular layer, making up the ascending portion of the axon (AA), then bifurcates at a right angle, forming two parallel fibres (PFs) that extend several millimetres along the folium. As a consequence, while an ascending axon can form multiple synapses with only a few overlaying PCs in the same sagittal plane as the granule cell soma, distributing information to a restricted number of cells, parallel fibres course through the dendritic trees of hundreds of PCs along the lobule (Napper & Harvey, 1988), distributing information widely and laterally. This morphology and functional data have suggested that Purkinje cell activity might be principally driven by local granule cells via the ascending axon synapses, while distant granule cells might modulate its activity via the parallel fibre system to provide the Purkinje cell with less specific contextual information.

In the adult rat, an estimated 175 000 excitatory PF synapses encode information on the dendritic tree of a single PC ((Napper & Harvey, 1988)). We previously identified two PF synaptic populations with

different molecular signatures ((Devi et al., 2016)), however, PF synapses have usually been treated as a uniform population, and we know little about the way the variety of information received by PCs is encoded at synaptic level. Isope and Barbour ((Isope & Barbour, 2002)) estimated that 85% of PF synapses are silent, as suggested by in vivo data ((Ekerot & Jörntell, 2001)), however that proportion was significantly lower for local granule cells and presumably AA synapses. In this study and that by Walter ((Walter et al., 2009)), properties of AA synapses were found to be indistinguishable from PF synapses. Sims and Hartell (2005) however, also compared AA and PF properties and showed that release probability is higher at AA synapses, endowing them with the capacity to transmit information more reliably at lower frequencies, while PF transmission requires higher frequency bursts. Also, AA synapses were refractory to plasticity with well described protocols, and they could neither induce associative CF-mediated LTD nor LTP ((Sims & Hartell, 2005);(Sims & Hartell, 2006)). These observations, together with the anatomical properties of the GC axon, prompted the conclusion that AA and PF synapses can transmit different types of information.

In this study we asked whether coincident activation of AA and PF synapses might be relevant to the PC, like associative activation with the CF, and trigger plasticity of GC inputs. We show that a protocol pairing stimulation of AAs and PFs, with inhibition preserved, results in long term synaptic plasticity of opposite sign of the two inputs, with potentiation of AA inputs and depression of PF inputs respectively, in a time-dependent manner. The dual plasticity we observe is dependent on NMDAR and mGluR activation, bringing together these two pathways and $GABA_AR$ activation also was required for efficient induction and maintenance of plasticity. Finally the plasticity does not rely on the differential distribution of AA vs PF inputs on the dendritic tree. We also examined the plasticity of the inhibitory component during this stimulation protocol.

Methods

Ethical approval: Sprague Dawley rats were provided by Janvier (St Berthevin, France) or bred and subsequently housed at the Animal Housing and Breeding facility of BioMedTech facilities (INSERM US36, CNRS UAR2009, Université Paris Cité) in agreement with the European Directive 2010/63/UE regarding the protection of animals used for experimental and other scientific purposes.

Experimental procedures were approved by the French Ministry of Research and the ethical committee

for animal experimentation of Paris Cité.

Slice preparation: Experiments were performed *in vitro* on horizontal slices 300 µm thick cut from the cerebellum of 19-25 day-old Sprague-Dawley male or female rats. Briefly, rats were killed by decapitation under general anaesthesia following inhalation of the volatile anaesthetic isoflurane at a concentration of 3-4% in accordance with the Directive 2010/63/UE and the cerebellum was quickly removed. After removal of the brainstem, the tissue was glued to the stage of a vibratome (Leica VT1200S, Germany). Slices were cut at a temperature of 34° C and subsequently kept in a vessel bubbled with 95% O_2 / 5% CO_2 at 34° C. Slice preparation and recordings were made in a bicarbonate buffered solution containing in mM: 115 NaCl, 2.5 KCl, 1.3 NaH_2PO_4, 26 $NaHCO_3$, 2mM $CaCl_2$, 1mM $MgSO_4$, 0.1mM Ascorbic Acid, and 25 glucose.

Patch-clamp recording of synaptic currents: Whole-cell patch-clamp recordings were made from Purkinje cells, identified by their size and location at the edge of the molecular and granule cell layers, with an EPC10 amplifier (HEKA, Germany) and PatchMaster acquisition software. The internal solution contained in mM: 135 KGluconate, 10 K_2 Creatine Phosphate, 10 HEPES, 0.01 EGTA, 2.5 $MgCl_2$, 2 $ATPNa_2$ and 0.4 GTPNa, pH adjusted to 7.3 with KOH and osmolarity to 295 mOsm/kg. When filled with the internal solution, recording pipettes had a resistance between 3 and 4.0 MΩ. Membrane currents were recorded at a pipette potential of -60 mV (not corrected for junction potential of approximately -12 mV pipette-bath). Series resistance was 80-90 % compensated. During experiments, the preparation was visualised on an upright microscope (Olympus BFX51; 60x 0.9 NA water dipping objective) and the bath was continuously perfused at a rate of 6 ml/min (6 bath volumes per min) with solution equilibrated with 95% O_2 / 5% CO_2 to maintain pH and solution recirculated.

Plasticity of granule cell to PC synapses was studied in horizontal cerebellar slices at a temperature of 30-32C. Horizontal slices were chosen as they better preserve PFs running in the plane of cut. Moreover, at this age, granule cell synapses are well established (Ichikawa et al., 2016). Parallel fibres and ascending axons were stimulated with a patch pipette slightly larger than those for recordings filled with a Hepes-buffered external solution and positioned either in the molecular or the granule cell layer as discussed in the result section. The baseline amplitude of both AA and PF pathways were sampled with a pair of suprathreshold pulses at 50 ms interval, delivered every 10 s (Fig 1A middle panel, stimulation was biphasic, 100-180 µs duration, 5 to 15V intensity constant voltage). The AA and PF test stimuli were separated by 0.5 s. In most of the experiments AAs were tested first to avoid

possible interference from mGluRs activation and the release of endocannabinoid by PFs. No antagonist was applied to the preparation, preserving the inhibitory inputs to the cell. Evoked responses consisted of EPSCs that were often quickly followed by IPSCs. The low Cl^- concentration in the intracellular solution ensured the reversal potential for Cl^- was close to the value determined for PCs (-85 mV, (Chavas & Marty, 2003)), and IPSCs were outward at the recording potential of -60 mV. On average, the amplitude of the AA-EPSC during baseline recordings was 110 ±12 pA and PF-EPSC 480 ±100 pA (n = 25), and the paired pulse ratio (PPR) was PPR_{AA} 1.93 ±0.08 and PPR_{PF} 1.89 ±0.07. After recording a baseline period of at least 10 minutes, we applied a stimulation protocol aimed at inducing plasticity. The recording configuration was switched to Current clamp and the potential set near -65 mV. The protocol applied (see Fig. 1A bottom panel, as in Ekerot & Jörntell, 2001 and Binda et al., 2016) consisted in the synchronous stimulation of both inputs by a train of 15 pulses at 100 Hz repeated every 3 s a total of 100 times. Following the induction protocol, the recording configuration was returned to Voltage clamp mode and test of alternate AA- and PF-EPSC amplitude resumed.

Analysis: For the analysis of synaptic currents, raw current traces were exported to Igor Pro (Wavemetrics) and peak excitatory current amplitudes were measured as the minimum over a time window overlapping the peak and spanning a few sampling points.

Compensation for rundown: The data sets presented Fig. 1C and D showed a pronounced run down of the baseline EPSC amplitude as compared to the experiments with simultaneous stimulation, where rundown stabilised during baseline (Fig 1B and supplementary Fig. 2A). While the baseline rundown implies that AA-LTP is likely more pronounced than we measured, PF-LTD could be overestimated. To better visualise LTD, in supplementary Fig. 2B to D we show the same set of data compensated for rundown. The time course of rundown was estimated by fitting the baseline of the normalised amplitude with an exponential and extrapolated for the duration of the experiment. The data was compensated for accordingly. Supplementary Fig. 2B shows little effect of the compensation on AA-LTP and PF-LTD when stimulating AAs and PFs simultaneously. However, supplementary Fig. 2C shows that the depression of PF inputs observed when stimulating AAs only was mostly due to rundown, and there was little AA-LTD. Supplementary Fig. 2D shows that there was no significant decrease of the AA-EPSC and a moderate PF-LTD when stimulating PFs only.

Chemicals: 2-(3-Carboxypropyl)-3-amino-6-(4methoxyphenyl)pyridazinium bromide (SR 95531), D-(-)-2-Amino-5-phosphonopentanoic acid (D-AP5) and 7-(Hydroxyimino)cyclopropa[b]chromen-1a-

carboxylate ethyl ester (CPCCOEt) were purchased from Tocris Bioscience or from HelloBio (UK). CPCCOEt was dissolved in DMSO to a concentration of 100mM and then diluted 2000x in saline just before use. All other stocks were prepared in water, and diluted in saline just before use. All other chemicals were purchased from Sigma.

Analysis of excitatory and inhibitory components of the evoked PSCs. A separate set of experiments were conducted to extract the excitatory and inhibitory component of the mixed PSC response evoked by stimulation of the fibres. We first recorded the AA- and PF- mixed EPSCs-IPSCs for a short control period and then applied SR95531 (3µM) for 3-4 mins. SR was then washed off the slice for 15 to 20 min, after which the induction protocol was applied, and the synaptic response was monitored for a further 30 min. SR was applied again to monitor the isolated EPSCs at the end of the experiment. On average, the plasticity of the AA- and PF-EPSC measured in these experiments was not significantly different from that in control experiments (AA pathway: 160 ± 30 %, as compared to 131±7 % in control, p=0.4,N=7 et N=24 and PF pathway 65 ± 9 %, as compared to 65 ± 5 % in control, p=1, N=7 et N=25 for SR and control respectively; ratio of normalised AA/PF responses: 3±1, p=0.76, N=7 et N=24), showing that the short applications of $GABA_AR$ antagonist did not influence the plasticity outcome (Fig. 4A). Similarly, the decrease in PPR of both inputs after induction was still observed. The pharmacologically-isolated EPSCs (measured between 2 to 3 min after SR perfusion) were used to characterise the kinetic parameters of the excitatory and inhibitory responses. The mixed PSCs were fitted with the sum of two synaptic functions with different onset delay and kinetics.

The EPSC component was fitted with a function of the form:

f(x)=0 for x<xd1

f(x) =A (1-exp(x-xd1)/tr1)^3*exp(x-xd1)/td1 for x>xd1

where x represents time and A, xd1, td1 and tr1 are the fitting parameters. A is the amplitude coefficient, xd1 the response delay after stimulus onset, tr1 the rise time constant of the third power exponential rise and td1 the decay time constant of the EPSC. We used a third power exponential rise as it best fitted the data compared to a single or quadratic exponential rise.

The IPSC component was fitted with a function of the form:

f(x)=0 for x<xd2

$f(x)=B\ (1-\exp(x-xd2)/tr2)^2*\exp(x-xd2)/td2$ for $x>xd2$

where x is time and B, xd2, td2 and tr2 are the fitting parameters. B is the amplitude coefficient, xd2 the response delay after stimulus onset, tr2 the rise time constant of the second power exponential rise and td2 the decay time constant of the IPSC. For the IPSC a quadratic exponential rise gave a good fit. The values of the fitting parameters for the excitatory synaptic function were obtained from the fit of the average response between 2 and 3 min (average of 6 traces) after beginning SR perfusion, when the inhibitory component was blocked. The fitted function was then subtracted from the mixed response recorded just before SR application to extract the inhibitory component. $GABA_AR$ inhibition had an effect on the EPSC amplitude, as already shown (Stell et al., 2007). For this reason the EPSC function was first rescaled to match the rise of the mixed response before subtraction. The inhibitory component was then fitted to estimate the kinetic parameters. The average values we found for the baseline responses in the 7 experiments were: average delay: 1.09±0.05 msec for excitatory (N=7) and 2.6±0.1 msec for inhibitory (N=6) responses for AA stimulation, and 1.16±0.08 msec for excitatory (N=7) and 2.9±0.2 msec for inhibitory (N=4) responses for PF stimulation; tau-decay: 5±1 msec for excitatory (N=7), 6.5±1.6 msec for inhibitory (N=6) responses for AA stimulation and 4.4±0.6 msec for excitatory (N=7) and 5±1 msec for inhibitory (N=4) responses for PF stimulation.

The average mixed PSC trace was fitted by the sum of the excitatory and inhibitory synaptic functions with fixed kinetic parameters to estimate the amplitude coefficients. The minimum and maximum of the excitatory and inhibitory fitting functions were used as an estimate of the real excitatory and inhibitory peak amplitudes. The excitatory and inhibitory fitting functions obtained for the first application of SR were used to calculate the amplitude of the synaptic components during the period preceding induction (10 min), and those obtained from the second SR application at the end of the recordings, to calculate the amplitudes after induction (30 min).

Statistical significance was tested with non-parametric methods for most of the data sets. These do not require assumptions about the nature of the distribution of the variables (as parametric tests do);we used either the Wilcoxon signed rank test (non-parametric, for paired samples) or the Wilcoxon Mann Whitney test (non-parametric, for unpaired samples). The T-test was used for control data only, where the N was big enough to show a normal distribution of the variables (see Supplementary figure 1). Tests were conducted using Igor Pro (Wavemetrics). All values given are mean ± SEM.

Results

Associative plasticity of AA synapses. To test the associative plasticity between ascending axon and parallel fibre inputs we positioned two separate stimulating electrodes to achieve activation of different granule cell inputs onto a Purkinje cell that was recorded with a third electrode in whole-cell configuration (Fig. 1A top panel). To stimulate PFs, a stimulation pipette was positioned in the molecular layer, 100 to 200 µm away from the dendritic tree of the recorded cell. The average length of a PF is between 4.2 and 4.7 mm ((Pichitpornchai et al., 1994)), therefore the vast majority of fibres stimulated in the molecular layer belong to GCs distant from the recorded cell. The probability that the stimulated fibres belong to GCs with somas lying close to the PC soma making AA synapses with the PC is of 1-2% percent. To stimulate AAs, a second stimulation pipette was positioned in the granule cell layer, within a narrow window centred on the PC somato-dendritic plane. The GCs stimulated in this position have a high probability of making ascending axon synapses onto the dendritic tree of the PC, although a small proportion could also make synapses from the proximal portion of PFs after bifurcation. For the sake of simplicity, we will use the terms AA and PF synapses thereafter although the terms proximal and distal synapses (with respect to GC soma) might be more appropriate.

The amplitude of AA and PF pathways were sampled with a pair of pulses (Fig 1A middle panel). Inhibitory inputs were preserved, and EPSCs were often followed by outward IPSCs. After baseline recording, a protocol aimed at inducing plasticity was applied (synchronous stimulation of both inputs by a train of 15 pulses at 100 Hz, every 3 s, 100 times, in Current clamp, see Fig. 1A bottom panel). Test of the AA and PF amplitude was then resumed. Figure 1A middle panel shows an example experiment with average traces of the AA-EPSC, in blue, and the PF-EPSC, in orange, 5 min before (continuous line) the plasticity induction protocol, and 25-30 min after the protocol (dotted line). Subtraction traces (25-30 min - last 5 min) are shown in grey to highlight changes. The AA-EPSC amplitude is increased while the PF-EPSC amplitude is decreased. Figure 1B top panel shows the time course of 24 such experiments for the AA pathway and 25 for the PF pathway with amplitude normalised to the last 5 minutes of control before plasticity induction. It shows that on average, following the induction protocol, we observed a long term change of opposite sign of the two inputs. The AA peak EPSC amplitude increased to 162 ±15% of baseline immediately after the induction protocol and then slowly decayed within 15 mins to stabilise at a value of 131 ± 7 % on average 25 to 30 minutes after induction, significantly larger than the baseline (p=7e-5 one-tailed T-test, n=24). The PF-EPSC on the other hand was almost unchanged immediately after the protocol (91 ±9%) and decreased to 65 ±5 % of baseline on average at

25-30 min, significantly smaller than the baseline (p=1e-7 one-tailed T-test, n=25). The level of plasticity measured in a given input pathway did not depend on the amplitude of the synaptic response of that input nor on the sum of the amplitudes of the two pathways (see supplementary Fig. 1), which could indicate that this plasticity is not cooperative, or that even relatively small inputs can sum up during repetitive stimulation to significantly depolarize the cell. We thus analysed the average number of spikes and the time at which the first spike took place during the first 5 trains of stimulation in the induction protocol. All cells except one did spike, even those with relatively weak synaptic currents for the first evoked response. The outcome of the plastic change for the AA EPSC only slightly correlated with the number of spikes and the time to the first spike, and no correlation was observed for PFs LTD (see supplementary Fig. 1).

While the peak amplitude of the first response in the pair of stimulations showed a progressive decline, the peak amplitude of the second response of both AA and PF underwent either LTP or LTD respectively, and was relatively stable thereafter. Figure 1B bottom panel shows that the paired pulse ratio of normalised amplitudes (PPR) of both pathways is transiently decreased following induction , but returns to its original value within 25-30 minutes. This suggests a transient presynaptic effect on release probability and likely explains the progressive effects on AA and PF responses. Fig 1B middle panel shows the ratio of normalised AA and PF peak amplitudes. The plot highlights the relative amplitude change of AA and PF inputs and eliminates changes common to both pathways as the transient change of PPR and rundown of synaptic responses. On average the relative amplitude of the normalised AA-EPSC more than doubles compared to that of the PF-EPSC, due to both the increase of the AA peak amplitude and the concomitant decrease of the PF. This relative amplitude change is sustained (normalised relative change : 2.5 ± 0.4 with N = 24, p=3e-4 after 25-30 mins of induction).

To test whether the plasticity observed is due to the co-activation of AA and PF inputs or the specific properties of the stimulated inputs, we performed a series of experiments in which either pathway was stimulated using the same induction protocol, but without the simultaneous stimulation of the other pathway. Figure 1C depicts the average behaviour in 8 experiments where only the AA pathway was stimulated during induction. The average amplitude of the AA-EPSC progressively decreased to 72 % ± 7% (N = 8) of control 25-30 minutes following the protocol, similarly to the PF-EPSC (64 % ± 6% of control, N = 8), both significantly smaller than baseline (p=0.008 for AA and p =0.004 for PF, N=8). The relative amplitude of the AA pathway was not significantly modified after the induction protocol (AA/PF 120 ± 20% after 25-30 min, p =0.58, N = 8, Fig. 1C bottom panel). This shows that stimulation of the AA

pathway alone is not sufficient to trigger AA-LTP.

On the other hand, Figure 1D shows the average result of 13 experiments where only the PF pathway was stimulated during induction. In this case, the AA pathway showed a small depression (84 ± 7 % of baseline after 25-30 min, N = 12, significantly different from baseline, p=0.009, N=12) whereas the PF pathway developed a larger depression over time (64 ± 6 % of baseline, significantly different from baseline, p=0.0002, N=13). Stimulation of the PF pathway on its own therefore appears to be sufficient to trigger PF-LTD of the same amplitude as in paired stimulation experiments (p=0.5). The relative amplitude of the AA pathway (AA/PF) doesn't change significantly after induction but slowly increases during the following 30 min (normalised AA/PF =140± 10 % of control, N = 12), which is in line with the progressive depression of the PF pathway. In these experiments, the PPR of the AA and PF pathways were transiently modified after induction, as in control, but only for the pathway stimulated during the protocol (see Fig. 1C and 1D bottom panel).

The baseline EPSCs were often affected by rundown (Figure 1B to D). While this implies that AA-LTP is likely more pronounced than we measured, PF-LTD on the other hand could be overestimated. In supplementary Fig. 2B to D, we show the same data compensated for rundown (see methods). While suppl. Fig. 2B shows little effect of the compensation on AA-LTP and PF-LTD when stimulating AAs and PFs simultaneously, suppl. Fig. 2C shows that the depression of PF inputs when stimulating AAs only was mostly rundown, and suppl. Fig. 2D shows little decrease of the AA-EPSCs when stimulating PFs only.

Stimulation of either pathway independently did not induce AA-LTP, showing that co-activation of AA and PF inputs is necessary and AA-LTP is associative. Compensating for baseline rundown indicated that PF-LTD is likely associative as well.

Timing dependence of plasticity. As the motor command always precedes reafferent sensory inputs, we tested the effect of the relative timing of stimulation of the AA and PF pathways on plasticity to determine if there was a timing dependence to the plasticity induction. During the induction protocol, the AA input was stimulated 150 ms after or 150 ms before the PF input. Figure 2A shows that when stimulating the AAs 150 ms after the PFs, the amplitude of the AA- and PF-EPSCs was depressed to a similar extent (AA was 53 % ± 15 % and PF 50 % ± 20 % of baseline, n = 8, not significantly different from each other p = 0.84). These changes were significantly different from experiments with synchronous

stimulation (p = 0.0002 for AA and p = 0.044 for PF). The relative amplitude of the AA pathway did not change significantly (AA/PF was 190 % ± 70 % of baseline, n = 7). On the other hand, when stimulating the AAs 150 ms before the PFs (see Fig. 2B), the amplitude of the AA-EPSC was first facilitated and declined back to baseline (AA was 100% ± 30%, n = 7, significantly different from synchronous stimulation p = 0.011), and the amplitude of the PF-EPSC was now close to baseline (84 % ± 12 %, n= 7, p = 0.062 for difference from synchronous stimulation). Given the clear baseline rundown of the PF pathway in this set of experiments, this decrease is closer to an absence of effect on PF-EPSC. The relative amplitude of the AA pathway was not facilitated significantly (AA/PF was 130 % ± 30 % of baseline), while the PPR was not affected (PPR_{AA} = 114 % ± 6 %, PPR_{PF} = 107 % ± 5%, N = 7).

Figure 2C shows that on average, the AA-EPSC was 131% ± 7% (N = 24) of baseline 25 to 30 min after the induction protocol when AA and PF stimulation was synchronous. It was 53% ± 15% (N = 8, p= 0.0002, significantly different from synchronous stimulation) of baseline when AA stimulation was given 150 ms after PF stimulation, and 97 % ± 26 % (N = 7, p = 0.022, not significantly different from synchronous stimulation) when the PF stimulation was started 150 ms after AA stimulation. The PF-EPSC was 65 % ± 5 % (N = 25, significantly different from AA, p = $6e^{-11}$) when stimulation was synchronous, 50% ± 20% (N = 8, p = 0.044, not significantly different from PF simultaneous stimulation) when AA stimulation was delayed by 150 ms, and 84 % ± 12 % (N = 7, p = 0.12, not significantly different from PF simultaneous stimulation) when PF stimulation was delayed by 150 ms.

These experiments show that the relative timing of the AA and PF input stimulation determines the extent of plasticity of both GC synapses, sometimes in opposite directions. Depending on the relative order and timing, the AA-EPSC was either facilitated or depressed significantly. Also and unexpectedly, PF-LTD was influenced by prior stimulation of the AA inputs.

Plasticity induction mechanism. PF-LTD and LTP have been linked to mGluR ((Daniel et al., 1992); (Konnerth et al., 1992); (Hémart et al., 1995)) and/or NMDAR activation ((Casado et al., 2002); (Bidoret et al., 2009); (Bouvier et al., 2016); (Kono et al., 2019)), and KOs of either receptor show defects in cerebellar learning ((Aiba et al., 1994); (Nakao et al., 2019); (Kono et al., 2019); (Schonewille et al., 2021)). mGluRs are highly expressed by PCs and located postsynaptically at GC to PC synapses. mGluRs activation requires PF train stimulation, however it has not been observed when stimulating sparse GC synapses ((Marcaggi & Attwell, 2005)). mGluRs in PCs activate several downstream pathways including

IP_3-mediated Ca^{2+} release ((Finch & Augustine, 1998); (Takechi et al., 1998)), endocannabinoid production ((Maejima et al., 2001); (Brown et al., 2003)), activation of a slow EPSC ((Batchelor et al., 1997); (Tempia et al., 1998); (Canepari et al., 2001)) and modulation of Ca^{2+} and K^+ channels ((Kammermeier et al., 2000); (Hildebrand et al., 2009); (Niculescu et al., 2013)). NMDARs on the other hand are not expressed in rat PCs at the age investigated at GC to PC synapses. However, they are expressed by molecular layer interneurons ((Glitsch & Marty, 1999); (Duguid & Smart, 2004)) and GCs ((Bidoret et al., 2009); (Bidoret et al., 2015)), where they are located on dendrites and presynaptic varicosities. Activation of presynaptic NMDARs has been shown to be involved in PF-LTD and LTP ((Casado et al., 2002); (Bidoret et al., 2009);(Bouvier et al., 2016)). We investigated the requirement for mGluR and NMDAR activation in induction of associative plasticity of the AA and PF pathways.

Figure 3A shows the effect of inhibiting NMDARs with the NMDAR competitive antagonist APV (50 µM) on associative AA and PF plasticity induction. APV was applied at the beginning of the recording. With NMDARs blocked, AA-LTP observed after synchronous stimulation was completely suppressed. The AA- and PF-EPSCs were on average 50% ± 5 % and 40% ± 2% of baseline 25 to 30 minutes after induction (n = 6, significantly different from control p = 3.4e-6, and n = 7, not significantly different from control p = 0.054 respectively). When compared to the PF pathway, depression was not significantly different at AA synapses and the relative amplitude of the AA pathway was increased to 109% ± 2% (n = 6) at 30 min. APV did not affect the transient depression of the PPRs. These data show that NMDAR activation is required for the associative AA-LTP described here.

In figure 3B, mGluRs were blocked using the competitive mGluR1 antagonist CPCCOEt (50 µM). In these conditions, the AA-EPSC increased transiently following the induction protocol, but there was a long term decrease within 25-30 minutes (AA was 72 ± 13 % of baseline, statistically smaller than control, p=0.0004, N=7 et N=24). PF-LTD was not blocked by the antagonist; if anything, there was an increase of LTD (PF was 54 ± 8 %, N=7, not significantly smaller than control, p=0.12, N=7). The transient decrease in PPR was present for both inputs, indicating no involvement of the mgluR1.

These results show for the first time the concomitant involvement of both mGluRs and NMDARs in the induction of plasticity at GC synapses.

Overlapping excitation and inhibition. Our experiments were all performed with inhibition intact and

with a Cl^- reversal potential close to the value estimated in PCs (-85 mV, (Chavas & Marty, 2003)). Because GCs also synapse on molecular layer interneurons, most of the time AA and PF stimulation recruits monosynaptic excitation and disynaptic inhibition to PCs, generating a mixed synaptic response with excitatory and inhibitory currents of opposite signs, and inhibition delayed. As a result, the time course of the recorded mixed PSC can be complex and excitation difficult to visualise. Moreover, our estimate of the peak EPSC amplitude and plasticity might not be accurate. To demonstrate that the complex shape of currents was due to the late onset of inhibition and control for possible errors in the estimate of the excitatory peak amplitude, in a set of experiments we made short applications of the $GABA_AR$ antagonist SR95531 (SR) before and after induction to isolate the excitatory from the inhibitory component of the synaptic response. Figure 4B shows for both AA and PF the average time course of the mixed response, and the extracted excitatory and inhibitory components, normalised to the baseline peak EPSC (see methods)(n=7 cells). This analysis was conducted for each cell, estimating the peak amplitudes, onset time and decay of excitatory and inhibitory synaptic responses. On average, the inhibitory component of both the AA- and PF-PSCs was shifted in time by more than 1 msec (average delay between inhibitory and excitatory current onset : 1.51±0.15 msec for AA stimulation, and 1.7±0.3 msec for PF stimulation). The decay time of the excitatory response was similar for both pathways (5±1 msec for AA and 4.4±0.6 msec for PF). We then analysed the change in amplitude of the two separated components after the induction protocol. Fig 4C shows an example of analysis of excitatory and inhibitory peak amplitudes before and after the induction protocol, with mixed traces and corresponding excitatory and inhibitory fitting functions, which shows an increase of the AA-EPSC and a decrease of the PF-EPSC, together with an increase of the IPSC in both pathways. Figure 4C bottom panel compares, for each cell, the AA- and PF-EPSCs relative amplitudes obtained by direct measure with those obtained with the fitting method. The delayed onset of the inhibitory component limits its impact on the EPSC amplitude, and the average level and sign of plasticity are not different from those obtained by the more refined fitting method (LTP of AA: 160± 30 % from fit vs 160± 30 % measured, p=0.9 of equal distributions; LTD of PF: 70± 10 % from fit vs 65± 9 % measured, p=1 of equal distributions).

In these experiments, the inhibitory disynaptic component evoked by both AA and PF stimulations had a tendency to increase after the pairing protocol (supplementary figure 3), indicating that excitation and inhibition do not necessarily change in the same direction. However, due to the small sample and the absence of an inhibitory component in some of the experiments, the level of long term changes in the inhibitory synaptic components was not significantly different from baseline (average change in peak

IPSC: 130± 50 % for the AA pathway, p=0.4 of being bigger than baselineN=5; and 150± 50 % for the PF pathway, p=0.2 of being bigger than baseline, N=4).

Role of inhibition. PCs receive GABAergic inhibition from molecular layer interneurons directly recruited by GCs, which is visible to different degrees in our recordings. $GABA_A$Rs are also present on GCs including presynaptically on the GC axon ((Stell et al., 2007)). These presynaptic $GABA_A$Rs are activated by synaptic release of GABA and affect the axonal Cl^- concentration and synaptic release ((Stell et al., 2007); (Astorga et al., 2015); (Berglund et al., 2016)). Several recent studies have shown that plasticity of PF-EPSCs is affected by GABAergic inhibition. Binda et al. (2016) showed that PF-LTP in mice relies on $GABA_A$R activation to hyperpolarize PC dendrites and allow recruitment of T-type Ca^{2+} channels. Rowan et al. (2018) also showed that the recruitment of molecular layer interneuron mediated inhibition can modify CF-mediated Ca^{2+} signal and LTD induction, turning LTD into LTP when MLIs are strongly recruited optogenetically.

The role of $GABA_A$Rs was tested during plasticity induction. To this end, a series of experiments was performed with the $GABA_A$R antagonist SR95531 (3 µM) present throughout, and the AA and PF pathways were stimulated as in control (Fig. 5). With $GABA_A$Rs blocked, the AA-EPSC was initially facilitated after induction (170±30 %, N=9), but that potentiation decreased with time and was not significant after 25-30 minutes. The outcome of induction on the AA pathway was highly variable, as shown by the error bars (Figure 5), and in 2 out of 9 cells, the AA-EPSC was strongly depressed at 25-30 min. On average, AA-LTP was smaller than in control experiments, but given the variability observed, it was not significantly different from baseline, nor from control experiments (117±24 % after 25-30 minutes, p=0.65 for significance with respect to baseline, p=0.1 for being significantly smaller than control, N=9). PF-LTD on the other hand was significant at 25-30 min (56±10%, N=9, p=0.002) and was not significantly smaller than control values (p=0.19). The PF-EPSC depressed more slowly and the relative size of the AA pathway was stable. The PPR of both pathways was transiently decreased. GABAA-R activation therefore seems to be required for efficient induction and maintenance of this type of associative plasticity.

Role of synaptic inputs distribution. We have shown that paired stimulation of AA and PF triggers AA-LTP. AAs can make several synapses per axon, but these are sparsely distributed on the vertical axis of the PC dendritic tree up to the axon bifurcation point. On the other hand, because PFs are stimulated in

the molecular layer, they are stimulated as a dense beam of fibres and therefore a dense patch of synapses on the PC dendritic tree. We asked whether induction of AA-LTP is due to the sparse distribution of AA synapses or to the stimulation of AA inputs *per se*.

To test for the role of the sparse distribution of the inputs, a series of experiments was performed substituting local AA stimulation with granule cell layer stimulation at a distance of 100 to 180 µm from the recorded PC. In this configuration, granule cell layer stimulation recruits PF synapses sparsely distributed on the PC dendrites and cannot involve AA synapses. The induction protocol was then applied to the sparse PF pathway (PF-sparse), together with the dense pathway stimulated in the molecular layer (PF-dense) (see Fig. 6A). Figure 6B shows an example of this experiment. Traces show the PF-sparse and -dense EPSCs before and after the induction protocol and subtractions (grey) to highlight changes. 25 to 30 minutes after induction, both the sparse and dense EPSCs are reduced by 62.1% and 55.2% respectively. The IClamp response of the PC is shown during the first two trains of stimulation of the protocol (Fig. 6A bottom panel). Fig. 6C shows the average time course of the experiment for 5 cells. Both the sparse and dense inputs are reduced on average to 65.1 % ± 14.6% of baseline (significantly different from control, $p = 0.0014$, n= 5 PF-sparse and n= 24 AA control) and 39.1% ± 5.9 % of baseline (not significantly different from control, $p = 0.013$, n= 5 PF-dense and n = 25 PF control) after 25-30 minutes respectively. When AA stimulation was replaced by sparse PF stimulation, the amplitude of the PF-sparse input was subsequently depressed over the following 30 minutes, with a time course similar to that of the PF-dense input. There was initially no change of relative amplitude of the two pathways, although with time, the dense PF input stimulated in the molecular layer was more strongly depressed than the sparse input, and the relative amplitude of PF-sparse increased to 177.4 % ± 39.2 % of baseline.

Experiments show that associative LTP of the AA input is not due to the sparse distribution of stimulated AA synapses on PC dendrites, but to the stimulation of a population of synapses prone to a specific form of plasticity.

Discussion

We show for the first time that stimulating AA and PF inputs simultaneously triggers LTP of the stimulated AA inputs specifically and LTD of PF inputs. AA-LTP is associative as it is not observed with

stimulation of either pathway alone and it is timing-dependent. AA-LTP is weakly dependent on GABAergic inhibition, but most interestingly also, on the activation of both mGluRs and NMDARs. It is linked to the identity of AA synapses rather than their sparse distribution on PC dendrites, as it is not observed for sparse PF inputs. Below we discuss these findings and potential consequences for our understanding of cerebellar physiology.

Identification of AA synapses. We have argued earlier that our approach for stimulating fibres recruits mainly PF synapses, for molecular layer stimulation, and mainly AA synapses, for local granule cell layer stimulation. We show in Fig. 6 that the difference in the plasticity outcome between the two inputs is not linked to the distribution of synapses on the dendritic tree but to different properties of the two populations. However, we have no morphological identification to verify that these are strictly AA or PF synapses. This is the limitation of our approach. Strictly speaking, granule cell layer stimulation will recruit proximal synapses, close to the soma of GCs, including some formed by the PF close to the bifurcation point of the axon, whereas molecular layer stimulation will recruit mostly synapses distal from the GC somas. Alternatively, there could be a gradient of properties from proximal to distal sites. If there is a gradient however, it is limited to short distances compared to the total fibre length, as this effect was not observed when stimulating PFs in the GC layer 100-180 µm from the recorded cell (4 to 5% of the total fibre length, Fig. 6). If the plasticity described here applies to a gradient along the GC axon rather than to AAs and PFs, this would not impact the mechanisms identified nor the consequences for cerebellar physiology.

AA plasticity. To our knowledge, only Sims and Hartell (2005, 2006) examined plasticity at AA synapses and reported the absence of both LTP and LTD associated with CF conjunctive stimulation. We have observed AA-LTP with synchronous stimulation and AA-LTD when AAs were stimulated in isolation or 150 ms after PFs (Fig. 2). Also, activation of both mGluRs and NMDARs is required for AA-LTP (Fig. 3). This is interesting in view of the past involvement of these receptors independently in cerebellar PF plasticity, both linked to PF stimulation**.** The difference with previous reports lies with the simultaneous stimulation of AA with a PF beam. We have not studied the downstream mechanisms involved, but a number of studies have investigated the role of presynaptic NMDARs and mGluRs in cerebellar LTD and LTP ((Daniel et al., 1992); (Konnerth et al., 1992); (Hémart et al., 1995); (Lev-Ram et al., 1997); (Casado et al., 2002); (Bidoret et al., 2009); (Bouvier et al., 2016)). NMDAR and mGluR activation could in principle take place at AA and PF synapses independently. However, the need for coincident activation of the two synaptic inputs suggests a requirement for crosstalk between the two synaptic territories and

for a signal not generated at AA synapses, at least when stimulated on their own. Crosstalk could happen either through spatial overlap or signal propagation between the inputs. Our experiments used horizontal slices, where PC dendrites dip into the slice, so we have no indication whether the two synaptic territories overlap. Given the size of the inputs (suppl. Fig. 1) however, spatial overlap is unlikely to happen in a significant proportion of experiments. This suggests that a signal needs to propagate from PF synapses.

As for the mechanism of coincidence detection, one possibility is that NMDARs or mGluRs are absent from AA synapses. We have no information on the specific localisation of receptors at AA vs PF synapses. mGluR-mediated Ca^{2+} signals are not expected to propagate across the PC dendritic tree, because both Ca^{2+} and IP3 are quickly buffered, and would be an unlikely substrate for crosstalk. mGluRs activation however, also triggers the production of endocannabinoids (EC), which can diffuse across membranes, and CB1Rs have been involved in PF-LTD ((P. K. Safo & Regehr, 2005); (Carey et al., 2011)). Similarly, presynaptic NMDARs have been linked to LTD through release of NO which also diffuses across membranes. The NO signal generated by PF activation might be sufficient to diffuse to the AA territory. PF-LTD has been shown to spread to nearby synapses ((Wang et al., 2000)). EC and NO are both potential substrates for crosstalk between AA and PF synapses, particularly as they diffuse across membranes.

Another possibility is that one receptor is present but fails to activate when AAs are stimulated on their own. The mGluR slow EPSC does not activate with sparse stimulation ((Marcaggi & Attwell, 2005)), which was attributed to insufficient build up of glutamate to activate the receptor. Canepari and Ogden (2006), however, showed that mGluR mediated Ca^{2+} release from stores is activated at lower glutamate concentration than the slow EPSC, and might therefore take place with sparse inputs, but importantly it requires prior priming by depolarisation. Fluctuations of the dendritic potential triggered by the PF-EPSC could enable mGluR mediated signals at AA synapses. There is no reason however for this mechanism to distinguish sparse AA from sparse PF inputs, unless the isolation of AA synapses in specific fine dendritic branches ((Lu et al., 2009)) makes them more prone to depolarisation.

PF-LTD. In the experimental conditions used here, PF-LTD was induced by the co-stimulation induction protocol. It was however difficult to separate from the rundown of synaptic responses. Baseline rundown amplified LTD, but in our opinion, the data suggest that PF-LTD is real and associative, like AA-LTP. Compensating for rundown indicated that isolated stimulation of one pathway did not trigger

significant LTD nor LTP (suppl. Fig. 2). This opinion is reinforced by the observation that when shifting the timing of presentation of the AA and PF inputs by 150 ms (Fig. 2C), the amplitude of the PF-EPSC was maintained rather than depressed. This is the only experimental condition where we did not observe a decrease of PF amplitude, making it unlikely that it is a spurious observation, and it indicates a clear impact of AA activation over the PF-EPSC

PF-LTD was unexpected because the induction protocol we used, when applied to PF only, was previously shown to induce PF-LTP in acute cerebellar slices ((Binda et al., 2016)) and rely on GABAergic inhibition. Our experiments were also performed with inhibition intact, and we show that LTP was reduced in the presence of SR, but we do not have an explanation for this difference with the study of Binda (2016). Noticeable differences with this study are the use of mice rather than rats, but also differences in the orientation of cut of the slices, which might have resulted in the study of different cerebellar lobules. Importantly also, we used a low internal Cl^- concentration, reproducing the concentration estimated in PCs (Chavas and Marty, 2005), and shifting the Cl^- reversal potential about 20 mV more hyperpolarised.

Role of inhibition. Experiments were performed with inhibition preserved and $GABA_A$Rs activation was shown to secure efficient induction of AA-LTP (see Fig. 5). Block of $GABA_A$Rs did not suppress plasticity, but under these conditions plasticity was reduced and highly variable. This is important to stress as plasticity was long studied *in vitro,* and still is, with inhibition blocked, but inhibition indeed seems to interfere with plasticity induction ((Binda et al., 2016); (Rowan et al., 2018)). At this stage, we have no detail on the mechanism of influence of GABAergic inhibition. Binda et al. (2016) showed that hyperpolarisation by IPSCs relieves inactivation of T-type Ca^{2+} channels, themselves regulated by mGluR1, boosting Ca^{2+} signals and triggering PF-LTP. That mechanism would seem compatible with our results at AA synapses although we do not know whether it requires NMDARs activation.

AA synapses as a distinct population of GC synapses. Sims and Hartell (2005 and 2006) studied AA synaptic properties and plasticity, and highlighted differences with PF synapses. In particular, they did not observe LTD when pairing AA with CF stimulation. Our work suggests that the association with PF synapses might be more relevant to refining AA inputs than the CF. Anatomical data also suggest that a large proportion of AA synapses are targeted to specific fine branches of the PC dendrites and segregated away from CF and PF synapses ((Lu et al., 2009)). These and the present study suggest that AA synapses are a different population of GC synapses. The anatomical differences between AAs and PFs

might be coupled to molecular and functional differences, taking advantage of the geometric organisation of the cerebellar cortex to encode information. Plasticity of AA synapses will need to be further examined with respect to the CF and local inhibition.

Physiology. Importantly, this work shows that the CF is not the only key to associative plasticity in PCs. Despite the large dimensions of the PC dendritic tree and the small inputs involved, it shows that integration at the level of the PC dendrites only requires moderate inputs. Subthreshold signals generated by PF and AA inputs can spread and trigger plasticity. It is a surprise, given that associative plasticity of granule cell inputs has only been described in association with the powerful CF input, which triggers widespread depolarisation and Ca^{2+} increase.

We argued in the introduction that, as a consequence of morphology, AAs can only form synapses with a few PCs, while PFs course through and synapse with the dendrites of hundreds of PCs. AA synapses are suited to encode precise and selective information, while PF synapses can encode a variety of information and could efficiently represent context. This work comforts the idea that they are functionally different and might fulfil distinct roles with respect to the computation performed by the cerebellar cortex. The associative form of plasticity we describe is expected to increase the contrast between AA and PF inputs in a time dependent manner, reinforcing AA signals presented conjointly with PF, while attenuating PF and AA signals presented in isolation. The time dependence is of particular interest as it would allow for modification of the inputs in relation to the timing of presentation, as expected for motor and sensory feedback information, which require pertinent association. The initial data on inhibition presented here suggested that the inhibitory signal is also increased. It will be interesting to study inhibitory signals further in this context to see whether they participate in creating a negative image of the excitatory signals, as observed in cerebellar-like structures.

Acknowledgements We thank Brandon Stell for discussions on the manuscript. We thank the Animal Housing and Breeding facility and the Prototyping facility of BioMedTech facilities (INSERM US36, CNRS UAR2009, Université Paris Cité) for providing the animals used in this study and assistance with technical developments. The work was funded by ANR grants ANR-19-CE37-011-01 SpinoCereLoco and ANR-18-CE16-0010-01 RewardInhib.

Figure legend

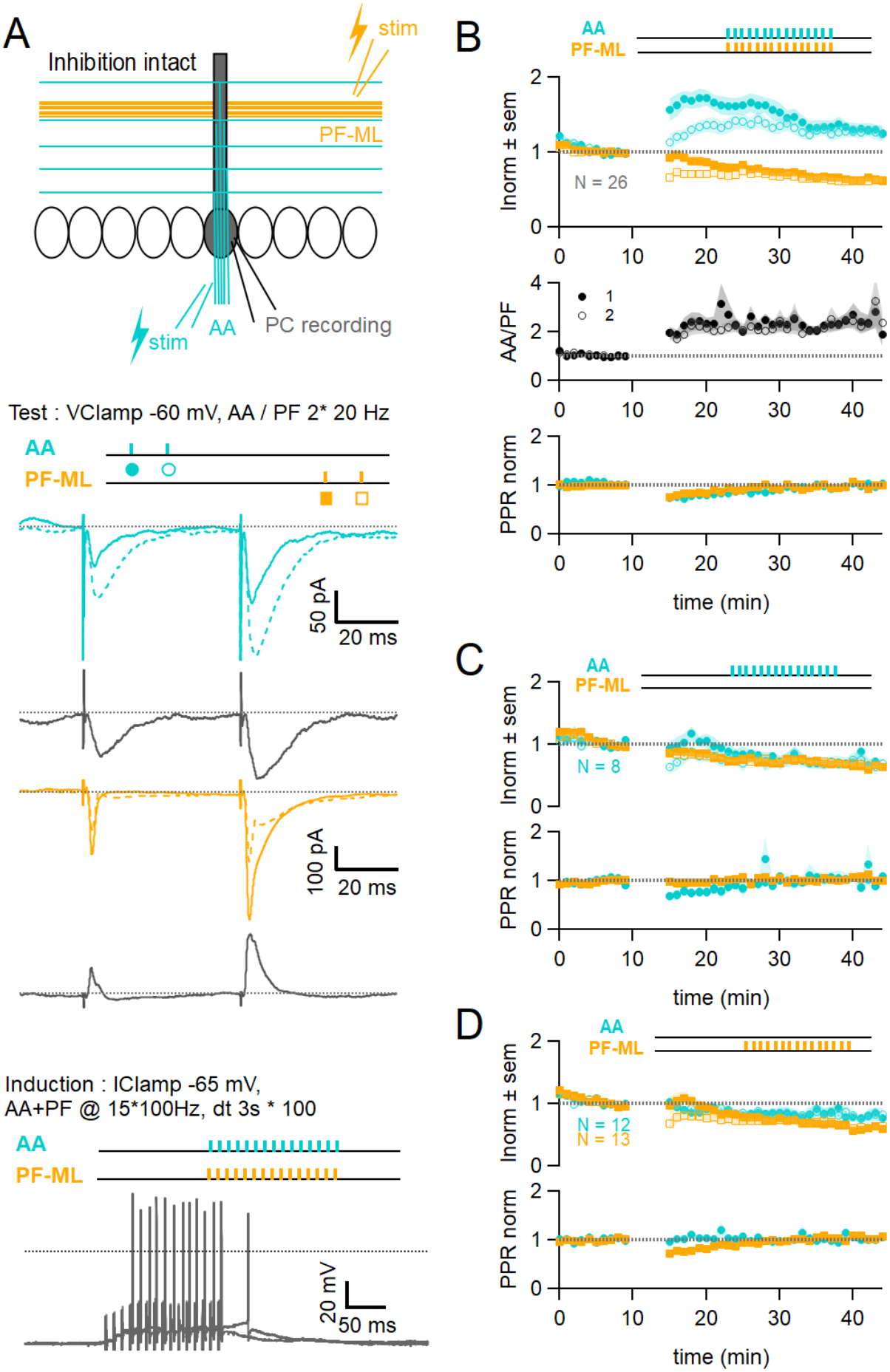
A
Inhibition intact
stim
PF-ML
stim
AA
PC recording
Test : VClamp -60 mV, AA / PF 2* 20 Hz
AA
PF-ML
50 pA
20 ms
100 pA
20 ms
Induction : IClamp -65 mV,
AA+PF @ 15*100Hz, dt 3s * 100
AA
PF-ML
20 mV
50 ms
B
AA
PF-ML
Inorm ± sem
N = 26
AA/PF
1
2
PPR norm
time (min)
C
AA
PF-ML
Inorm ± sem
N = 8
PPR norm
time (min)
D
AA
PF-ML
Inorm ± sem
N = 12
N = 13
PPR norm
time (min)

Figure 1: Associative plasticity of AA and PF inputs. A, top. Experimental configuration: whole cell patch-clamp recording in a PC with two stimulation electrodes positioned to activate different granule cell inputs. To stimulate PFs, a pipette was positioned in the molecular layer, 100 to 200 µm from the PC dendritic tree. To stimulate AAs, a second pipette was positioned in the granule cell layer, within a narrow window centred on the PC somato-dendritic plane (less than 50 µm). Evoked synaptic current recordings were performed in the voltage clamp mode, except during the induction protocol. **Middle**, The AA- and PF-EPSCs were sampled with a pair of pulses (dt = 50 ms), every 10 s, AA and PF test stimuli separated by 0.5 s. Sample traces from one experiment : average of the AA-EPSC (blue) and PF-EPSC (orange), before (5-10 min, continuous line) and after the induction protocol (25-30 min, dotted line). Subtraction traces (25-30 min - 5-10min) in grey. The AA-EPSC amplitude increased while the PF-EPSC amplitude decreased. No antagonist was applied to preserve the inhibitory inputs, and evoked responses often consisted of EPSCs quickly followed by IPSCs. IPSCs were outward at -60 mV. The irregular decay kinetics of the PF-EPSCs reveal the presence of an IPSC. **Bottom**, induction protocol. The recording configuration was switched to current clamp and the potential set near -65 mV. The AA and PF pathways were stimulated synchronously by a train of 15 pulses at 100 Hz every 3 s for 5 min. Grey traces show the current clamp recordings during the first two trains of stimulation. **B Top**, plot of the average AA (blue) and PF (orange) peak EPSC amplitude normalised to the last 5 minutes of baseline (n = 26, closed symbol: first response in the pair, open symbol: second response). Following the induction protocol, a long term change of opposite sign of the two inputs was observed. The peak amplitude of the AA-EPSC increased to 128 ± 7 % (N = 25) of baseline at 25-30 min after the induction, significantly larger than baseline (p=0.00035 one-tailed T-test, n=25). The PF-EPSC on the other hand decreased slowly to 65 ±5 % (N = 25) of baseline at 25-30 min, significantly smaller than baseline (p=1e-7 one-tailed T-test, n=25). **Middle**, average ratio of the normalised amplitudes of AA and PF inputs showing the relative changes of the two inputs. On average the relative AA-EPSC amplitude doubles, and that increase is sustained. **Bottom**, the average normalised paired pulse ratio (PPR = AA2/AA1 and PF2/PF1) is transiently decreased following induction.**C.** Average time course of 8 experiments with stimulation of the AA pathway only during the induction protocol. **Top**, on average, the amplitudes of AA- and PF-EPSCs normalised to the last 5 minutes of baseline (colours and symbols as in A) progressively decreased to 72 % ± 7% (N = 8) and 64 % ± 6% (N = 8) respectively at 25-30 minutes, both significantly smaller than baseline (p =0.004 for AA and PF, N=8). This shows that stimulation of the AA pathway alone is not sufficient to trigger AA-LTP. **D.** Average result of 13 experiments where only the PF pathway was stimulated. **Top**, the AA normalised EPSCs showed a small and steady depression (84 ± 7 % of baseline

after 25-30 min, N = 12, significantly different from 100%, p=0.009, N=12) whereas the PF pathway developed depression over time (64 ± 6 % of baseline, significantly different from 100%, p=0.0002, N=1). Stimulation of the PF pathway on its own therefore appears to be sufficient to trigger PF-LTD. **C** and **D bottom**, the PPR of the AA and PF pathways transiently decreased, but only for the pathway stimulated during the induction protocol.

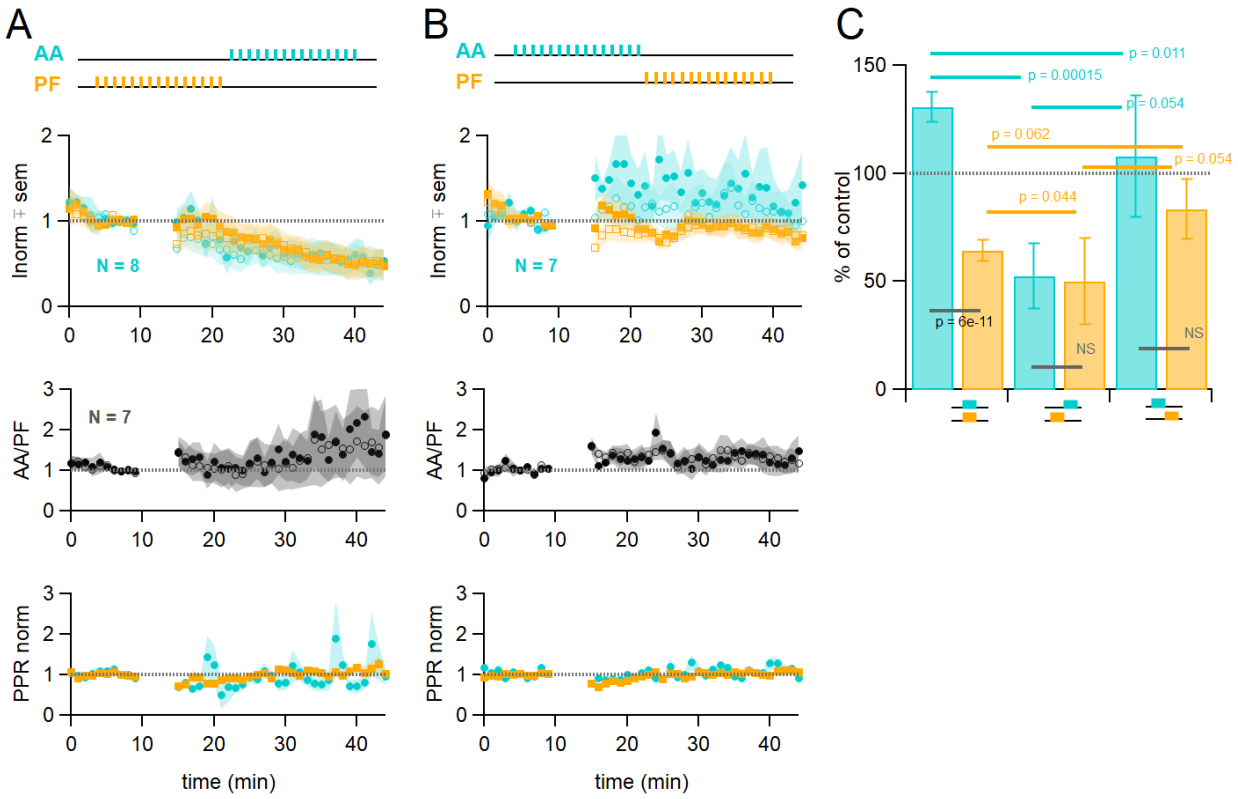

Figure 2: Time dependence of plasticity. The effect of the relative timing of stimulation of the AA and PF pathways on plasticity was tested by stimulating the AA input 150 ms after or 150 ms before the PF input. **A.** On average, when stimulating AAs 150 ms after PFs, the AA- and PF-EPSCs now decreased by an extent similar(AA was 52.6 % ± 15.0 %, PF 50.2 % ± 19.9 % of control, n = 8, not significantly different p = 0.84). These changes were significantly different from experiments with synchronous stimulation (p = 0.0002 for AA and p = 0.044 for PF). The relative amplitude of the AA pathway did not change significantly (AA/PF was 185.3 % ± 74.3 % of control, n = 7). **B.** When stimulating the AAs 150 ms before the PFs, the AA-EPSC was first facilitated, but declined back to control values (AA was 100% ± 30% of control, n = 7, significantly different from synchronous stimulation p = 0.011). The amplitude of the PF-EPSC was maintained close to baseline (PF 84 % ± 12 % of control, n= 7, p = 0.062 for difference from synchronous stimulation). The relative amplitude of the AA pathway was not facilitated significantly (AA/PF was 125.6 % ± 30.9 % of control), while the PPR was not affected (PPR_{AA} = 114.4 % ± 6.4 5, PPR_{PF} = 107.1 % ± 4.6%, N = 7, p = 0.375). **C.** Plot of average amplitude as a percentage of baseline: the AA-EPSC was 131% ± 7% (N = 24) 25 to 30 min after induction when AA and PF stimulation was synchronous. It

was 52.6% ± 15.0% (N = 8, significantly different from synchronous stimulation, p= 0.0.0002) of control when AA stimulation was 150 ms after PF stimulation and 97.0 % ± 26.1 % (N = 7, not significantly different from synchronous stimulation, p = 0.022) when PF stimulation was started 150 ms after AA stimulation. The PF-EPSC was 63.6 % ± 5.2 % (N = 15, significantly different from AA, p = $6e^{-11}$) when stimulation was synchronous, 50.2% ± 19.9% (N = 8, not significantly different from AA, p = 0.84; N = 8, p = 0.044, not significantly different from PF simultaneous stimulation) when AA stimulation was delayed by 150 ms, and 84.0 % ± 11.8 % (N = 7, not significantly different from AA, p = 1.06; not significantly different from PF simultaneous stimulation p = 0.123) when PF stimulation was delayed by 150 ms.

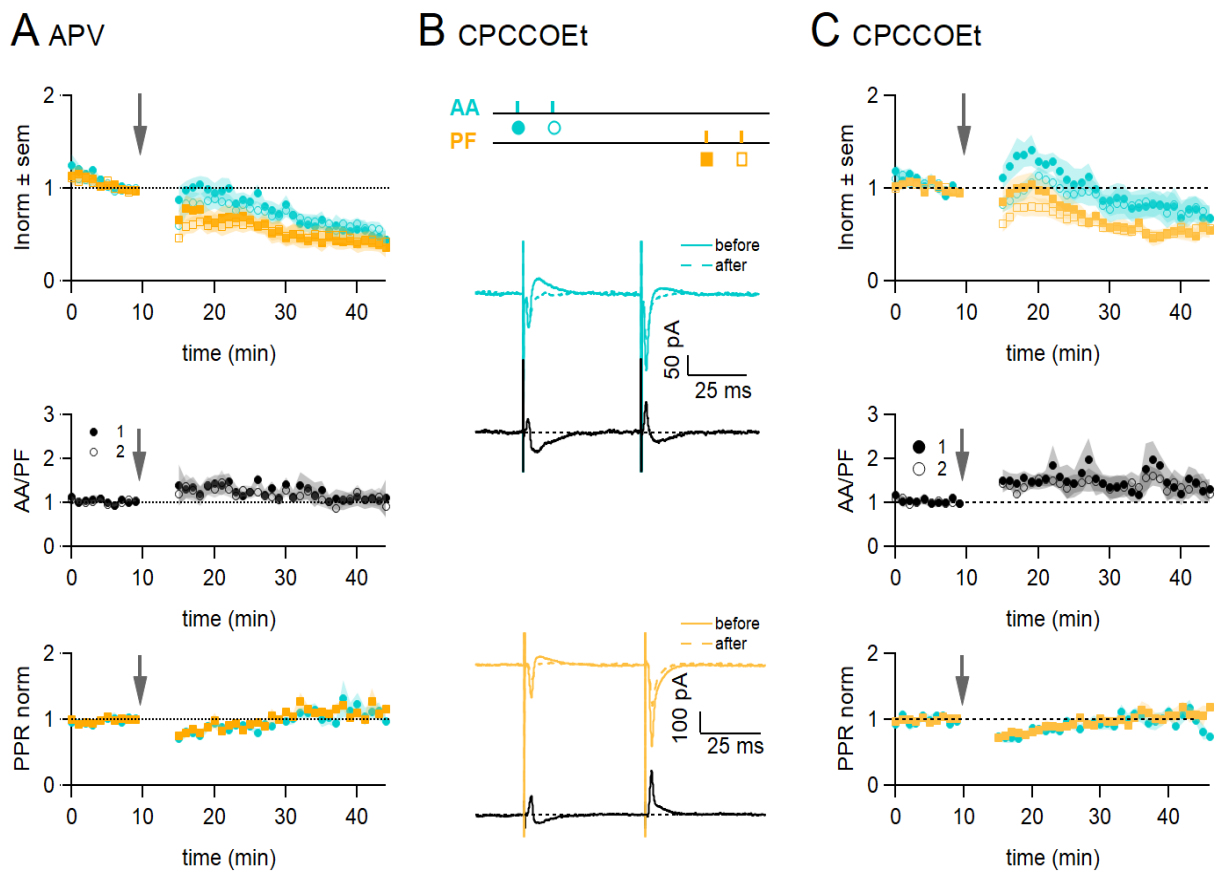

Figure 3: Role of NMDARs and mGluRs. A. Average of 7 experiments in the presence of the NMDAR competitive antagonist APV (50 µM). **Top**: Average normalised AA- and PF-EPSC amplitudes as a function of time (colours and symbols as in B, top). Following induction in the presence of APV, both AA and PF pathways were depressed, showing that NMDAR activation is necessary for AA-LTD induction. **Middle**: The relative amplitude of the AA pathway is slightly increased, reflecting a slower depression of the AA inputs. **Bottom**: the transient decrease of the normalised PPR is still observed. **B.** Bath application of CPCCOEt, a selective blocker of mGluR1Rs, strongly inhibits LTP of AA-EPSCs. Sample recordings from one experiment with CPCCOEt (50 µM). The traces are the average of the AA(blue) and PF (orange) synaptic responses, before (5-10 min, continuous line) and after induction (25-30 min, dotted line). Subtraction traces (25-30 min - 5-10min) in grey. No increase of the AA-EPSC is observed, while the PF-EPSC is decreased as in control experiments. **C. Top**: Average time course over 8 experiments of the normalised AA- and PF-EPSC. mGluR1 receptor block impairs LTP of the AA-EPSC. PF-LTD is instead preserved. Middle: as a result, a small sustained increase of the relative amplitude of AA-EPSC is observed. **Bottom**: as for APV, CPCCOEt does not influence the short term decrease in PPR after induction, as shown in the plot of the normalised PPR of both input pathways during recording.

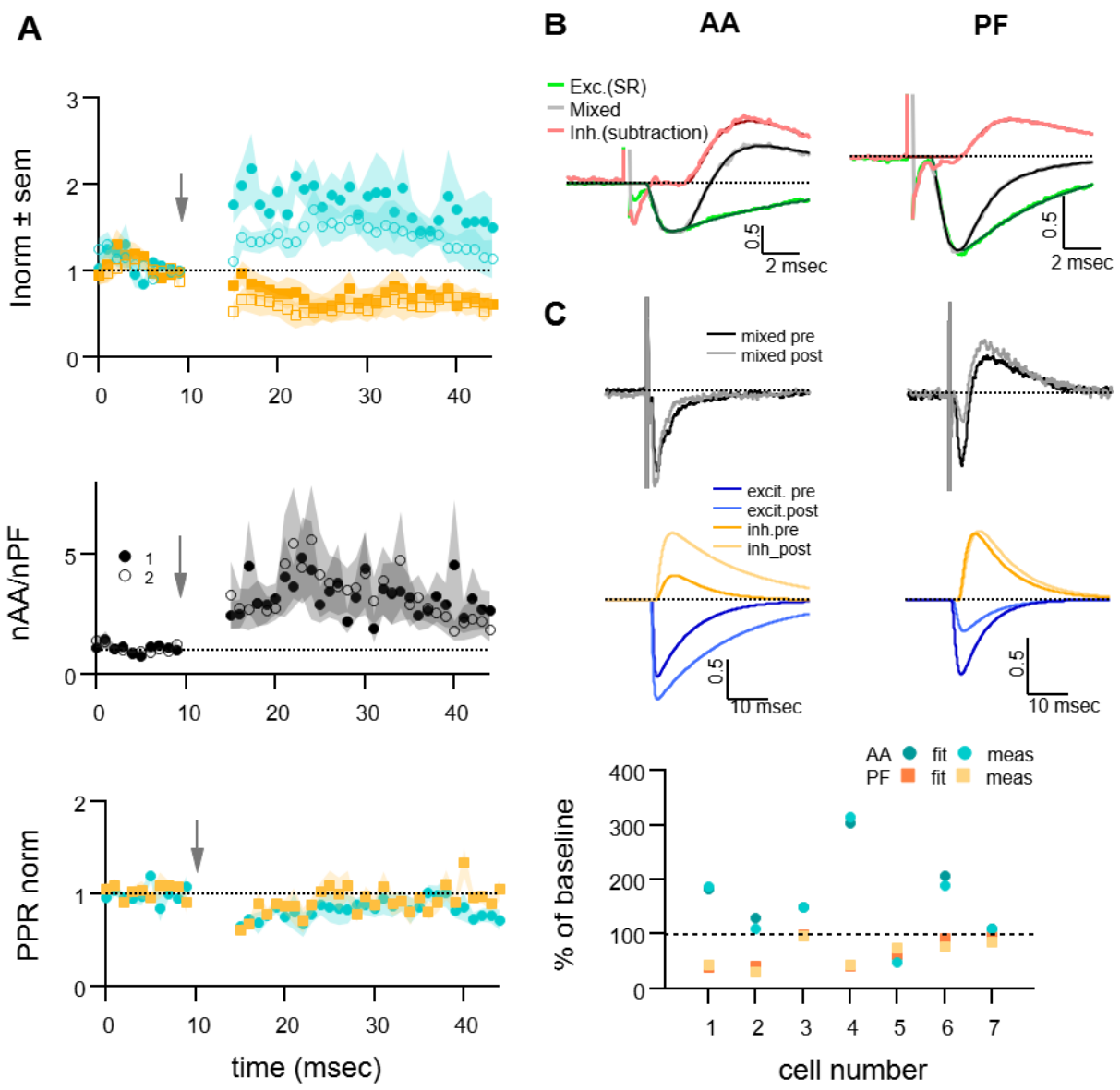

Figure 4: Dissecting excitation and disynaptic inhibition confirms the plastic changes of AA and PF EPSCs. A. Average results of 7 experiments in which gabazine (SR) was applied twice transiently (20 min before induction and 30 min after induction) to isolate the excitatory component of the response. Top: peak EPSCs amplitudes of the first and second evoked responses in the pair for both AA (blue, closed circles: first response in the pair, open circles: second response) and PF(orange, closed squares: first response in the pair, open squares: second response) stimulation. In the middle and bottom panel are shown the ratio of the normalised AA to PF amplitudes and the normalised PPR. The amplitude of the short and long term plastic changes are not different from those of control experiments. **B.** Examplification of the fitting procedure used to extract the excitatory and inhibitory components of the

recorded mixed PSCs, applied on the normalised traces averaged over all experiments. Traces were normalised to the absolute value of the peak excitatory baseline response and then averaged over all cells. To the left, the mixed evoked PSC measured right before induction (black) is shown together with the excitatory response recorded during the first SR application (green). The inhibitory trace is the difference between the mixed response and the fit of the excitatory response (red). On average inhibition was delayed and relatively smaller in amplitude for both AA and PF pathways. The excitatory and inhibitory fitting functions used to determine the kinetics of the two components are shown overlaid, as well as the mixed fitting function used to determine the amplitude coefficients of the components (dark thick lines). **C** Sample traces for an experiment where the excitatory and inhibitory components were extracted for both baseline mixed PSC and the mixed PSC recorded 25-30 mins after induction; top: mixed PSCs for AA (left) and PF (right) responses before and after induction; below are shown the corresponding decomposed excitatory (blue, dark and light for pre and post-induction respectively) and inhibitory components (orange, dark and light for pre and post-induction respectively). The AA-EPSC increased and the PF-EPSC decreased, while both AA- and PF-IPSCs increased in this example. Bottom: The EPSC amplitude relative to baseline at 25-30 mins after induction are compared for the two analysis methods for each cell. The plot shows the peak amplitude measured directly as the minimum from the recorded mixed response (meas) with that obtained as the minimum of the excitatory fitting function for each cell. Disynaptic inhibition only slightly affected the measure of the real excitatory peak, both for AA- (blue triangles) and PF-EPSC(orange circles) (AA measured:160 ± 30 %, from fit: 160 ± 30% and PF measured: 65 ± 9 %, from fit: 70 ± 10 %).

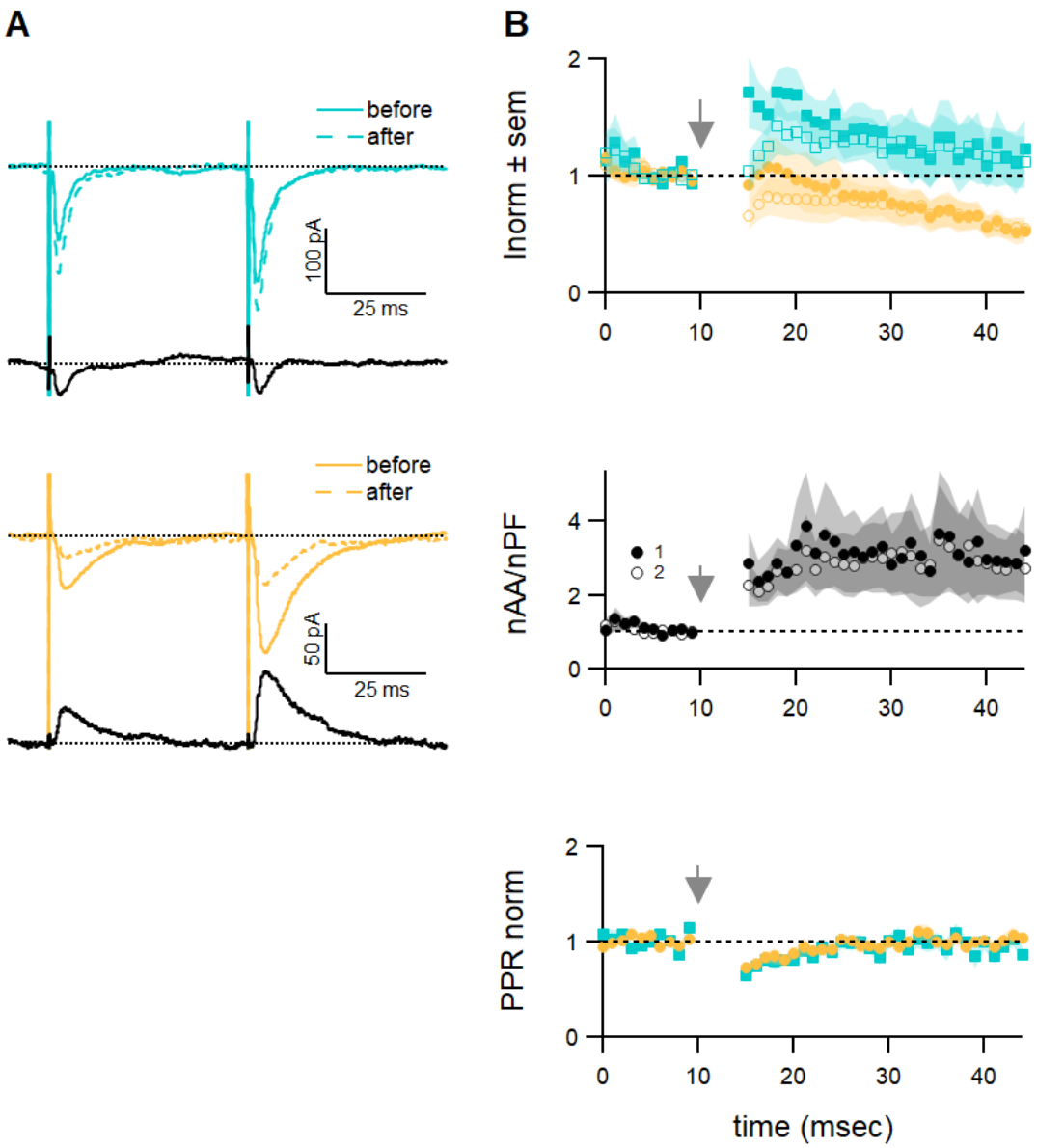

Figure 5: GABA$_A$ receptor block affects long term plastic changes. A. Sample recordings from an experiment with SR present throughout. Paired EPSCs evoked before and after induction, together with subtraction traces, are shown for the AA and PF pathways. The AA response is increased after induction and the PF response is strongly decreased in this experiment. **B.** Average peak EPSC amplitudes of the first and second evoked responses for both AA and PF of 9 experiments. The big errors in AA peak amplitude measured after induction are due to a large variability of the outcome of the protocol on this pathway (AA LTP:117±24 % ; PF-LTD: 56±10%, n = 9). The ratio of the normalised AA and PF amplitude shows the same variability, while the normalised PPR displays the same relative error and time course as control experiments.

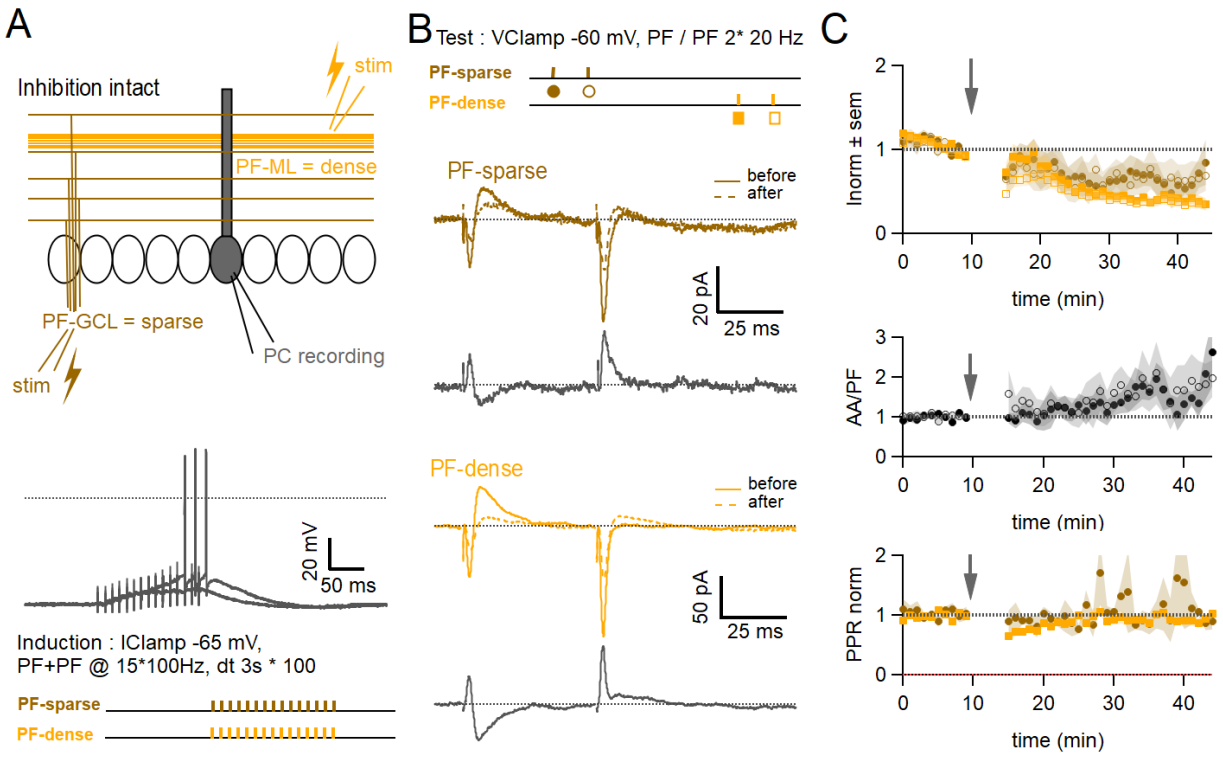

Figure 6: Role of the AA input sparse distribution. A. To test the role of the sparse input distribution, a stimulation electrode was positioned in the granule cell layer, 100 to 180 µm from the recorded PC, stimulating only PF synapses sparsely distributed on the PC dendrites. The induction protocol was applied to the sparse PF pathway (PF-sparse), together with the dense PF pathway stimulated in the molecular layer (PF-dense). **B.** Example experiment. Traces show the PF-sparse and -dense EPSCs before and after induction and subtractions (grey) to highlight changes. 25 to 30 minutes after induction, both the sparse and dense EPSCs are reduced by 35% and 43% respectively. **Bottom left**, IClamp responses to the first two trains of stimulation. **C.** Average time course of the experiment for 5 cells. Both sparse and dense inputs (colours and symbols as in B, top) are reduced on average to 65.1 % ± 14.6% (significantly different from control, p = 0.0027648, n= 5 PF-sparse and n= 25 AA control) and 39.1% ± 5.9 % of baseline (not significantly different from control, p = 0.0130942, n= 5 PF-dense and n = 25 PF control) after 25-30 min respectively. When AA stimulation was replaced by sparse PF stimulation, the amplitude of the PF-sparse input was depressed over the following 30 minutes, similarly to that of the PF-dense input. With time the dense PF input was more strongly depressed, and the relative amplitude of PF-sparse increased to 177.4 % ± 39.2 % of control.

References

Aiba, A., Kano, M., Chen, C., Stanton, M. E., Fox, G. D., Herrup, K., Zwingman, T. A., & Tonegawa, S. (1994). Deficient cerebellar long-term depression and impaired motor learning in mGluR1 mutant mice. *Cell*, *79*(2), 377–388.

Astorga, G., Bao, J., Marty, A., Augustine, G. J., Franconville, R., Jalil, A., Bradley, J., & Llano, I. (2015). An excitatory GABA loop operating in vivo. *Frontiers in Cellular Neuroscience*, *9*, 275. https://doi.org/10.3389/fncel.2015.00275

Berglund, K., Wen, L., Dunbar, R. L., Feng, G., & Augustine, G. J. (2016). Optogenetic Visualization of Presynaptic Tonic Inhibition of Cerebellar Parallel Fibers. *The Journal of Neuroscience: The Official Journal of the Society for Neuroscience*, *36*(21), 5709–5723. https://doi.org/10.1523/JNEUROSCI.4366-15.2016

Bidoret, C., Ayon, A., Barbour, B., & Casado, M. (2009). Presynaptic NR2A-containing NMDA receptors implement a high-pass filter synaptic plasticity rule. *Proceedings of the National Academy of Sciences of the United States of America*, *106*(33), 14126–14131. https://doi.org/10.1073/pnas.0904284106

Binda, F., Dorgans, K., Reibel, S., Sakimura, K., Kano, M., Poulain, B., & Isope, P. (2016). Inhibition promotes long-term potentiation at cerebellar excitatory synapses. *Scientific Reports*, *6*, 33561. https://doi.org/10.1038/srep33561

Bouvier, G., Higgins, D., Spolidoro, M., Carrel, D., Mathieu, B., Léna, C., Dieudonné, S., Barbour, B., Brunel, N., & Casado, M. (2016). Burst-Dependent Bidirectional Plasticity in the Cerebellum Is Driven by Presynaptic NMDA Receptors. *Cell Reports*, *15*(1), 104–116. https://doi.org/10.1016/j.celrep.2016.03.004

Canepari, M., & Ogden, D. (2006). Kinetic, pharmacological and activity-dependent separation of two Ca2+ signalling pathways mediated by type 1 metabotropic glutamate receptors in rat Purkinje neurones. *The Journal of Physiology*, *573*(Pt 1), 65–82. https://doi.org/10.1113/jphysiol.2005.103770

Carey, M. R., Myoga, M. H., McDaniels, K. R., Marsicano, G., Lutz, B., Mackie, K., & Regehr, W. G. (2011). Presynaptic CB1 receptors regulate synaptic plasticity at cerebellar parallel fiber synapses. *Journal of Neurophysiology*, *105*(2), 958–963. https://doi.org/10.1152/jn.00980.2010

Casado, M., Isope, P., & Ascher, P. (2002). Involvement of presynaptic N-methyl-D-aspartate receptors in cerebellar long-term depression. *Neuron*, *33*(1), 123–130. https://doi.org/10.1016/s0896-6273(01)00568-2

Chavas, J., & Marty, A. (2003). Coexistence of excitatory and inhibitory GABA synapses in the cerebellar interneuron network. *The Journal of Neuroscience: The Official Journal of the Society for Neuroscience*, *23*(6), 2019–2031.

Coesmans, M., Weber, J. T., De Zeeuw, C. I., & Hansel, C. (2004). Bidirectional parallel fiber

plasticity in the cerebellum under climbing fiber control. *Neuron*, *44*(4), 691–700. https://doi.org/10.1016/j.neuron.2004.10.031

Daniel, H., Hemart, N., Jaillard, D., & Crepel, F. (1992). Coactivation of metabotropic glutamate receptors and of voltage-gated calcium channels induces long-term depression in cerebellar Purkinje cells in vitro. *Experimental Brain Research*, *90*(2), 327–331. https://doi.org/10.1007/BF00227245

Devi, S. P. S., Howe, J. R., & Auger, C. (2016). Train stimulation of parallel fibre to Purkinje cell inputs reveals two populations of synaptic responses with different receptor signatures. *The Journal of Physiology*, *594*(13), 3705–3727. https://doi.org/10.1113/JP272415

Ekerot, C. F., & Jörntell, H. (2001). Parallel fibre receptive fields of Purkinje cells and interneurons are climbing fibre-specific. *The European Journal of Neuroscience*, *13*(7), 1303–1310. https://doi.org/10.1046/j.0953-816x.2001.01499.x

Finch, E. A., & Augustine, G. J. (1998). Local calcium signalling by inositol-1,4,5-trisphosphate in Purkinje cell dendrites. *Nature*, *396*(6713), 753–756. https://doi.org/10.1038/25541

Hémart, N., Daniel, H., Jaillard, D., & Crépel, F. (1995). Receptors and second messengers involved in long-term depression in rat cerebellar slices in vitro: A reappraisal. *The European Journal of Neuroscience*, *7*(1), 45–53. https://doi.org/10.1111/j.1460-9568.1995.tb01019.x

Ichikawa, R., Hashimoto, K., Miyazaki, T., Uchigashima, M., Yamasaki, M., Aiba, A., Kano, M., & Watanabe, M. (2016). Territories of heterologous inputs onto Purkinje cell dendrites are segregated by mGluR1-dependent parallel fiber synapse elimination. *Proceedings of the National Academy of Sciences of the United States of America*, *113*(8), 2282–2287. https://doi.org/10.1073/pnas.1511513113

Isope, P., & Barbour, B. (2002). Properties of unitary granule cell—>Purkinje cell synapses in adult rat cerebellar slices. *The Journal of Neuroscience: The Official Journal of the Society for Neuroscience*, *22*(22), 9668–9678. https://doi.org/10.1523/JNEUROSCI.22-22-09668.2002

Jörntell, H., & Ekerot, C.-F. (2002). Reciprocal bidirectional plasticity of parallel fiber receptive fields in cerebellar Purkinje cells and their afferent interneurons. *Neuron*, *34*(5), 797–806. https://doi.org/10.1016/s0896-6273(02)00713-4

Konnerth, A., Dreessen, J., & Augustine, G. J. (1992). Brief dendritic calcium signals initiate long-lasting synaptic depression in cerebellar Purkinje cells. *Proceedings of the National Academy of Sciences of the United States of America*, *89*(15), 7051–7055. https://doi.org/10.1073/pnas.89.15.7051

Kono, M., Kakegawa, W., Yoshida, K., & Yuzaki, M. (2019). Interneuronal NMDA receptors regulate long-term depression and motor learning in the cerebellum. *The Journal of Physiology*, *597*(3), 903–920. https://doi.org/10.1113/JP276794

Lev-Ram, V., Jiang, T., Wood, J., Lawrence, D. S., & Tsien, R. Y. (1997). Synergies and coincidence requirements between NO, cGMP, and Ca2+ in the induction of cerebellar long-term depression. *Neuron*, *18*(6), 1025–1038. https://doi.org/10.1016/s0896-6273(00)80340-2

Lu, H., Esquivel, A. V., & Bower, J. M. (2009). 3D electron microscopic reconstruction of segments of rat cerebellar Purkinje cell dendrites receiving ascending and parallel fiber granule cell synaptic inputs. *The Journal of Comparative Neurology*, *514*(6), 583–594. https://doi.org/10.1002/cne.22041

Marcaggi, P., & Attwell, D. (2005). Endocannabinoid signaling depends on the spatial pattern of synapse activation. *Nature Neuroscience*, *8*(6), 776–781. https://doi.org/10.1038/nn1458

Montgomery, J. C., & Bodznick, D. (1994). An adaptive filter that cancels self-induced noise in the electrosensory and lateral line mechanosensory systems of fish. *Neuroscience Letters*, *174*(2), 145–148. https://doi.org/10.1016/0304-3940(94)90007-8

Nakao, H., Kishimoto, Y., Hashimoto, K., Kitamura, K., Yamasaki, M., Nakao, K., Watanabe, M., Kano, M., Kirino, Y., & Aiba, A. (2019). MGluR1 in cerebellar Purkinje cells is essential for the formation but not expression of associative eyeblink memory. *Scientific Reports*, *9*(1), 7353. https://doi.org/10.1038/s41598-019-43744-z

Napper, R. M., & Harvey, R. J. (1988). Number of parallel fiber synapses on an individual Purkinje cell in the cerebellum of the rat. *The Journal of Comparative Neurology*, *274*(2), 168–177. https://doi.org/10.1002/cne.902740204

Pichitpornchai, C., Rawson, J. A., & Rees, S. (1994). Morphology of parallel fibres in the cerebellar cortex of the rat: An experimental light and electron microscopic study with biocytin. *The Journal of Comparative Neurology*, *342*(2), 206–220. https://doi.org/10.1002/cne.903420205

Rowan, M. J. M., Bonnan, A., Zhang, K., Amat, S. B., Kikuchi, C., Taniguchi, H., Augustine, G. J., & Christie, J. M. (2018). Graded Control of Climbing-Fiber-Mediated Plasticity and Learning by Inhibition in the Cerebellum. *Neuron*, *99*(5), 999-1015.e6. https://doi.org/10.1016/j.neuron.2018.07.024

Safo, P. K., & Regehr, W. G. (2005). Endocannabinoids control the induction of cerebellar LTD. *Neuron*, *48*(4), 647–659. https://doi.org/10.1016/j.neuron.2005.09.020

Safo, P., & Regehr, W. G. (2008). Timing dependence of the induction of cerebellar LTD. *Neuropharmacology*, *54*(1), 213–218. https://doi.org/10.1016/j.neuropharm.2007.05.029

Sawtell, N. B. (2017). Neural Mechanisms for Predicting the Sensory Consequences of Behavior: Insights from Electrosensory Systems. *Annual Review of Physiology*, *79*, 381–399. https://doi.org/10.1146/annurev-physiol-021115-105003

Schonewille, M., Girasole, A. E., Rostaing, P., Mailhes-Hamon, C., Ayon, A., Nelson, A. B., Triller, A., Casado, M., De Zeeuw, C. I., & Bouvier, G. (2021). NMDARs in granule cells contribute to parallel fiber-Purkinje cell synaptic plasticity and motor learning. *Proceedings of the National Academy of Sciences of the United States of America*, *118*(37), e2102635118. https://doi.org/10.1073/pnas.2102635118

Sims, R. E., & Hartell, N. A. (2005). Differences in transmission properties and susceptibility to long-term depression reveal functional specialization of ascending axon and parallel fiber

synapses to Purkinje cells. *The Journal of Neuroscience: The Official Journal of the Society for Neuroscience*, *25*(12), 3246–3257. https://doi.org/10.1523/JNEUROSCI.0073-05.2005

Sims, R. E., & Hartell, N. A. (2006). Differential susceptibility to synaptic plasticity reveals a functional specialization of ascending axon and parallel fiber synapses to cerebellar Purkinje cells. *The Journal of Neuroscience: The Official Journal of the Society for Neuroscience*, *26*(19), 5153–5159. https://doi.org/10.1523/JNEUROSCI.4121-05.2006

Stell, B. M., Rostaing, P., Triller, A., & Marty, A. (2007). Activation of presynaptic GABA(A) receptors induces glutamate release from parallel fiber synapses. *The Journal of Neuroscience: The Official Journal of the Society for Neuroscience*, *27*(34), 9022–9031. https://doi.org/10.1523/JNEUROSCI.1954-07.2007

Walter, J. T., Dizon, M.-J., & Khodakhah, K. (2009). The functional equivalence of ascending and parallel fiber inputs in cerebellar computation. *The Journal of Neuroscience: The Official Journal of the Society for Neuroscience*, *29*(26), 8462–8473. https://doi.org/10.1523/JNEUROSCI.5718-08.2009

Wang, S. S., Khiroug, L., & Augustine, G. J. (2000). Quantification of spread of cerebellar long-term depression with chemical two-photon uncaging of glutamate. *Proceedings of the National Academy of Sciences of the United States of America*, *97*(15), 8635–8640. https://doi.org/10.1073/pnas.130414597